1.3.2 Physics of low energy tail in the CCD response function

A response of the frontside illuminated CCDs to monochromatic X-rays shows a noticeable low energy tail in addition to the well understood main peak and escape and fluorescence features. It is generally assumed for silicon detectors that the tail's origin is due to dead layer on the surface of the device [21, 23]. We have studied the response of the CCD to the monochromatic synchrotron X-rays at BESSY in a wide range of energies and have discovered an unknown feature in the very low energy part of the response function (see [29, 28]). Examining changes in its behavior as a function of energy of incoming radiation we came to the conclusion that it originates from the photons interacting in the gate insulator, which is not a dead layer as was previously thought. We have developed a model that explains the shape of this newly discovered feature as well as the shape of entire low energy tail in the CCD response function.

1.3.2.1 Experimental

Experimental data were acquired at the electron storage ring BESSY (Berlin), where device cooled down to -120^o C was illuminated with monochromatized synchrotron X-rays. The data were taken at the KMC (Krystal MonoChromator) beamline in a wide range of energies from 1487 eV to 5898 eV with the emphasis on the understanding of the device behavior around silicon absorption K edge (1836 eV). That explains the choice of the energy data points for this measurement having higher density around silicon K edge: 1487, 1700, 1740, 1800, 1825, 1832, 1835, 1836.5, 1838, 1840, 1842, 1845, 1847, 1855, 1870, 1900, 2015, 2309, 2622, 3313, 3691, 4090, 4510, 4952, 5414, and 5898 eV. A typical exposure time at each energy was 4000 seconds, with 5 times that amount for the 2015 eV measurement.

Device was clocked by the ACIS electronics with serial register clock frequency of 100 kHz, total system noise at this frequency being about 2 electrons rms. Very low system noise was the crucial factor that allowed us to observe the low energy features discussed below.

1.3.2.2 Escape and fluorescence peaks

At X-ray energies greater than silicon K absorption edge, which we have measured for crystalline silicon to be 1839 eV, the response function of the device shows two distinct peaks in addition to the primary one. One of them at energy $E_f = 1739$ eV is due to the silicon fluorescent photons that have escaped far enough from the original site of interaction to be detected as a separate event. The other peak centered at energy $E_e = E_0 - E_f$, where E_0 is energy of the incident photon, is called an escape peak. It is formed by the electron clouds that are left when the flourescent photon carrying away energy E_f leaves silicon substrate or, again, is stopped far enough to be detected separately. The behavior of these peaks is reasonably well described by the model developed as a part of ACIS calibration program and is discussed in more detail in section 1.14. The relative amplitudes of these peaks as a function of energy, both experimentally measured and simulated, are shown in Fig. 1.128.

1.3.2.3 Low energy peak

On Fig. 1.8 is shown the histogram of the CCD response to the monochromatic flux of 1700

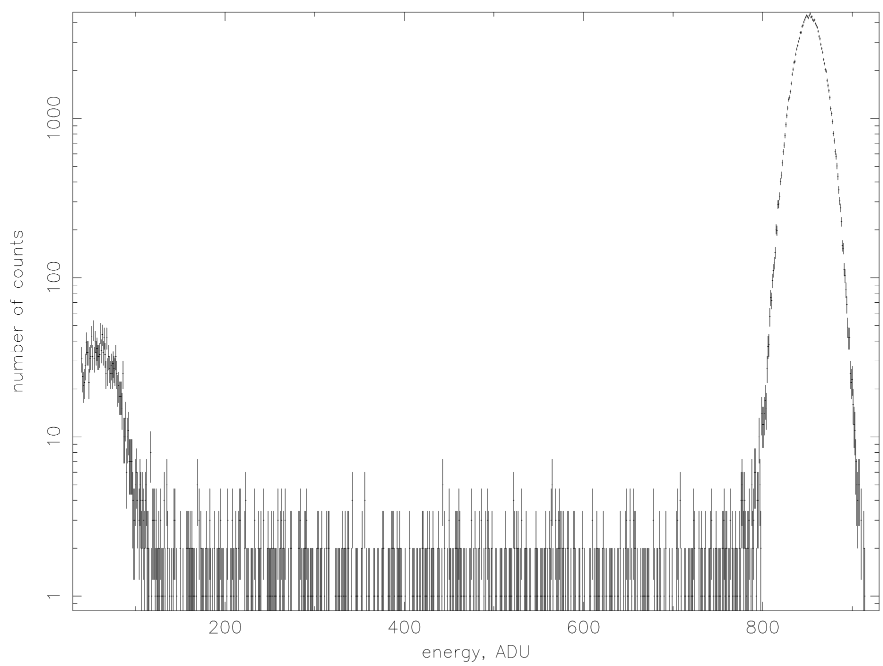

Figure 1.8: Histogram of the CCD response to 1700 eV X-rays.

eV X-rays, this histogram is typical for the device response at energies below the silicon absorption K edge (1841 eV). It has two distinct peaks - the main one which corresponds to the energy of the incoming photons, and the second one at energy which constitutes 7% of the main peak energy. Notice that since 1700 eV is below the silicon K absorption edge energy, silicon fluorescence does not play any role here.

The shape of the low energy peak is not quite gaussian, though it is possible to make a gaussian fit of reasonable quality. Having done that at different energies we found that the centroid of the low energy peak moves approximately proportionally to the centroid of the main peak (which is known to be a linear function of the energy of irradiating photons), as it is shown in Fig 1.9. Such behavior is different, for instance, from the silicon escape

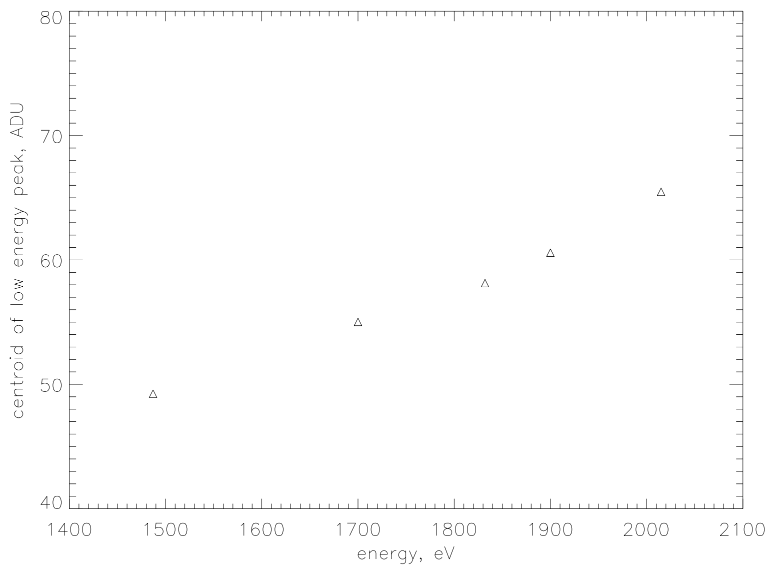

Figure 1.9: Centroid of the low energy peak as a function of energy.

peak for which energy shift is exactly the same as for the main peak.

Another important observation is that total number of counts in the low energy peak is consistent with the number of calculated photon interactions within the gate isolator.

If we assume that the gate insulator consists of a layer of SiO_2 with thickness d_{ox} and characteristic absorption length λ_{ox}, the number of photons per unit area N_{ox} absorbed in it is

$$N_{ox} = N_0(1 - \exp{(-\frac{d_{ox}}{\lambda_{ox}})}) \tag{1.6}$$

where N_0 is photon flux enetering SiO_2 layer. The number of photons N_{si} that are absorbed inside the volume of silicon and form the main peak in the histogram equals simply entire flux of photons entering silicon in the case when thickness of the depleted layer of silicon d_d is big compared to the characteristic absorption length in silicon λ_{si}. Due to attenuation in the gate oxide $N_{si} = N_0 \exp{(-\frac{d_{ox}}{\lambda_{ox}})}$. This gives the ratio of the intensities for the two peaks:

$$\frac{N_{ox}}{N_{si}} = (e^{\frac{d_{ox}}{\lambda_{ox}}} - 1) \tag{1.7}$$

In the case $d_{ox} \ll \lambda_{ox}$ which is definitely true at energies below silicon absorption K edge, formula (1.7) comes to

$$\frac{N_{ox}}{N_{si}} = \frac{d_{ox}}{\lambda_{ox}} \tag{1.8}$$

In Fig. 1.10 is shown the ratio of the number of events in the low energy peak to the number of events in the main peak as a function of energy. The dashed line in this Figure

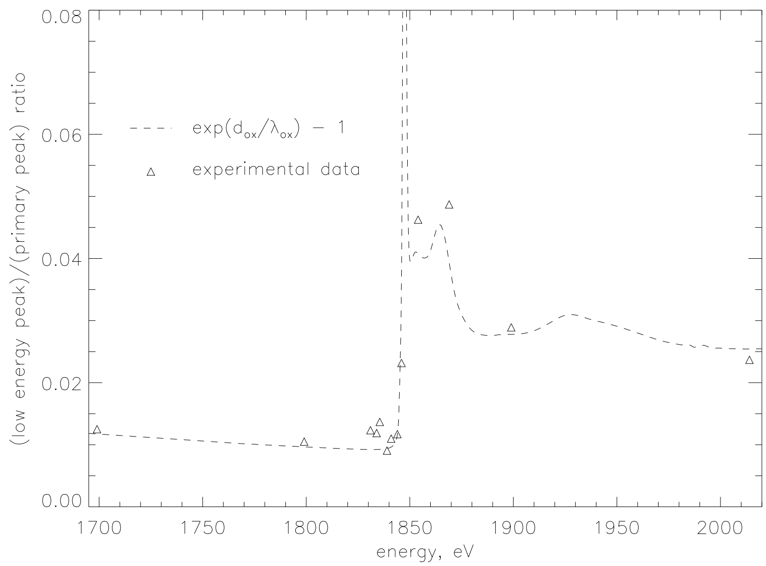

Figure 1.10: Ratio of number of counts in low energy peak and in the primary peak as a function of energy, calculated (dashed line), and measured (triangles).

is the result of the calculation according to equation 1.7. The dependence of λ_{ox} on energy comes from our high precision experimental measurement (see [25]) and includes all the details of the near edge absorption structure. The relative number of counts in the low energy peak jumps up sharply at the energy corresponding to the silicon K absorption edge, in full agreement with the prediction of the formula 1.7.

The most remarkable feature of this plot is that the jump occurs at the energy corresponding to the silicon absorption edge in SiO_2, which is different from the silicon absorption edge in the crystalline silicon. We have shown in [25] that there exists a 6 eV shift between the silicon absorption edge energies in Si and SiO_2. Three data points on Fig 1.10 in between the two edges staying at the same level as the points below the edge in Si prove most reliably that the low energy peak originates in the SiO_2 layer.

Unlike diode-type detectors such as Si(Li) [21] or $p\!-\!n$ junction CCD [23], buried channel CCDs have an electric field in the gate oxide covering silicon surface. In Fig. 1.11 is shown a distribution of the potential in the gate structure of the buried channel CCD. It is clear from this figure that electrons generated in the SiO_2 layer adjacent to the silicon substrate will be travelling towards the collecting potential well of the CCD. Charge created in the Si_3N_4 and other layers sitting on the top of it will be lost. The mobility of the electrons in silicon dioxide, although lower than in silicon by roughly an order of magnitude, is still high enough to allow the photogenerated charge to get collected in a frame time.

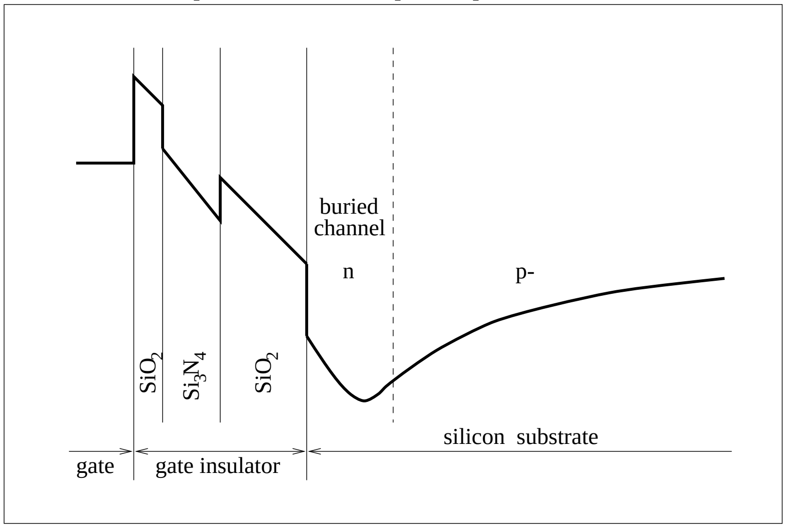

Figure 1.11: Potential distribution in the buried channel CCD.

All these facts lead to the unambiguous conclusion that the low energy peak's origin is due to the photons absorbed inside the gate insulator.

When an X-ray photon interacts with a material of the gate oxide layer, it generates a cloud of electron-hole pairs. Since the bandgap of SiO_2 is approximately 9 eV (as opposed to 1.12 eV in silicon), the amount of electrons created by one photon is approximately an order of magnitude lower than for silicon-absorbed photons. As a result the corresponding peak in a histogram is seen at very low energy.

So far we have discussed only data taken at energies around silicon K edge. The picture is very different at higher energies. At 5414 eV (a histogram of the device response is shown on Fig. 1.12) instead of the well-defined low energy peak shifted further up from what we see at 1700 eV histogram, there is a broad elevation which goes all the way down to the noise peak (not shown) without reaching a maximum. We believe that the reason for such behavior is an increased electron cloud size at higher energies. It is known that the diameter of an electron cloud generated by a photon increases with energy and according to various authors could be tens or even hundreds of nanometers at several keV [21, 23, 26]. The gate oxide layer is very thin, approximately 70 nm and its thickness is comparable to the cloud size. When the cloud diameter exceeds the oxide thickness, for any cloud originated in silicon dioxide part of the charge will end up either in silicon, or in silicon nitride and the amount of that charge depends on the photon's depth of interaction. There exists a potential barrier for the electrons that are moving from Si_3N_4 into SiO_2 (see Fig. 1.11), which means that part of the cloud that enters Si_3N_4 will be almost entirely lost.

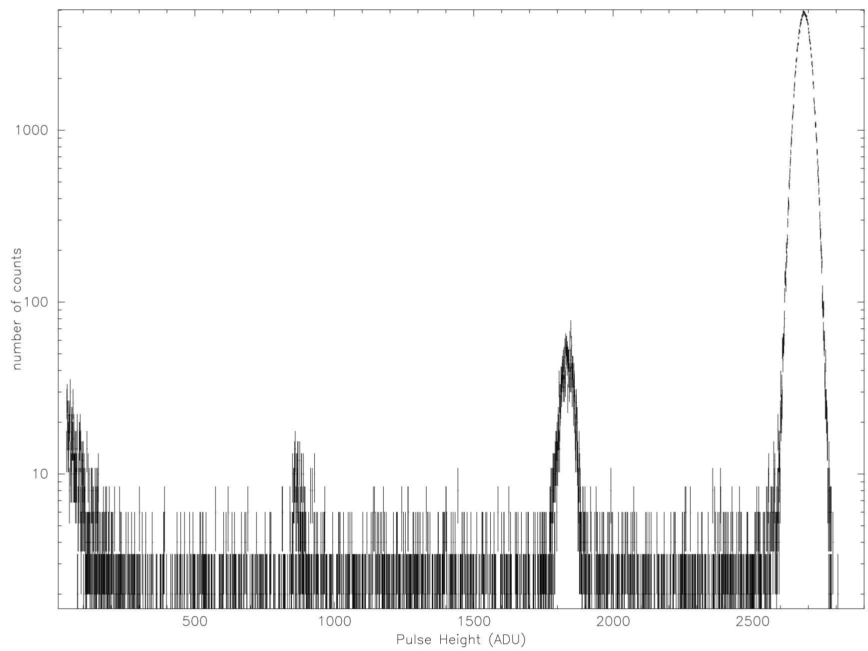

Figure 1.12: Histogram of the CCD response to 5414 eV X-rays.

For the events that originate in Si_3N_4 only electrons with sufficiently high enough energy can overcome the potential barrier.

Thus, even small changes in the depth of interaction of the original photon in the SiO_2 layer lead to significant changes in the total number of electrons collected, and as a result the low energy peak is washed out into a much broader feature without an extremum.

1.3.2.4 Shape of the entire low energy tail

A similar phenomenon - splitting of the electron cloud between silicon and silicon dioxide - should obviously take place for any cloud which originates within the distance R from the $Si - SiO_2$ interface, where R is the cloud radius. Since the number of the electron-hole pairs generated per eV of the incoming photon energy is significantly higher in silicon than in silicon dioxide, the amplitude of such events will change gradually from the primary peak down to the low energy peak, as the center of the cloud moves from silicon into oxide. This is schematically shown in Fig. 1.13, which explains how the low energy tail of the spectral redistribution function is formed. Fig. 1.14 provides evidence that the entire low energy tail comes from the photons interacting within a small distance from the silicon interface. This figure shows the fraction of the events in the tail as a function of the characteristic absorption length λ_{si} in silicon. In order to produce this plot events in the fluorescent and

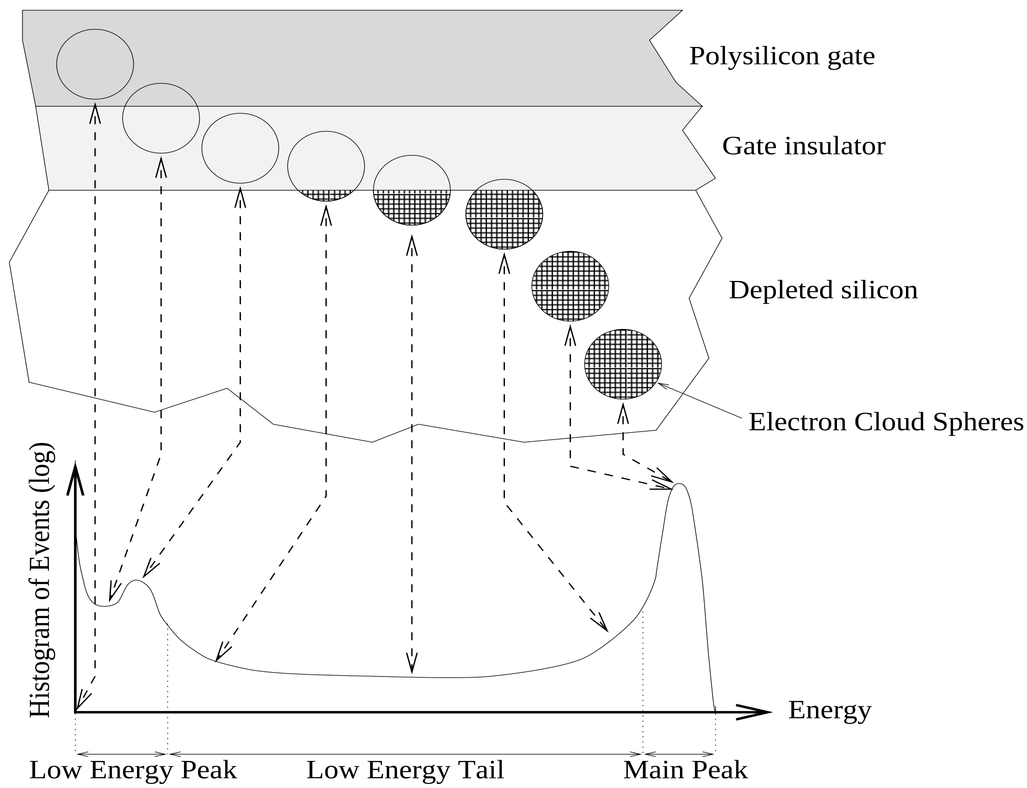

Figure 1.13: Scheme of forming low energy tail from the electron clouds generated close to $Si - SiO_2$ interface.

in the escape peaks were ignored, as well as the low energy (oxide) peak events discussed above. Each point in this plot corresponds to a measurement at a particular energy, and the points are connected sequentially in energy ascending order, starting at the lowest energy point labeled 1487 eV. The plot demonstrates that for widely separated energies (for instance, 1487, 1836, and 3600 eV) with the similar valaues of λ_{si} the fraction of events in the tail is similar. Moreover, immediately above the silicon edge, at very small λ_{si}, the tail intensity goes up sharply. If one makes a very crude assumption that the cloud radius R is constant (or slowly changing function of energy in the range of interest), then an approximately $1/\lambda_{si}$ dependence is an indication that the flat part of the tail results from the the photons interacting in a shallow region near the surface, whose thickness $2R$ is small compared to λ_{si}.

If all the events in the flat part of the low energy tail come from the electron clouds formed within a distance R from the $Si - SiO_2$ interface, the fraction of the events in the flat part of the tail can be used to determine the electron cloud size. The results of such

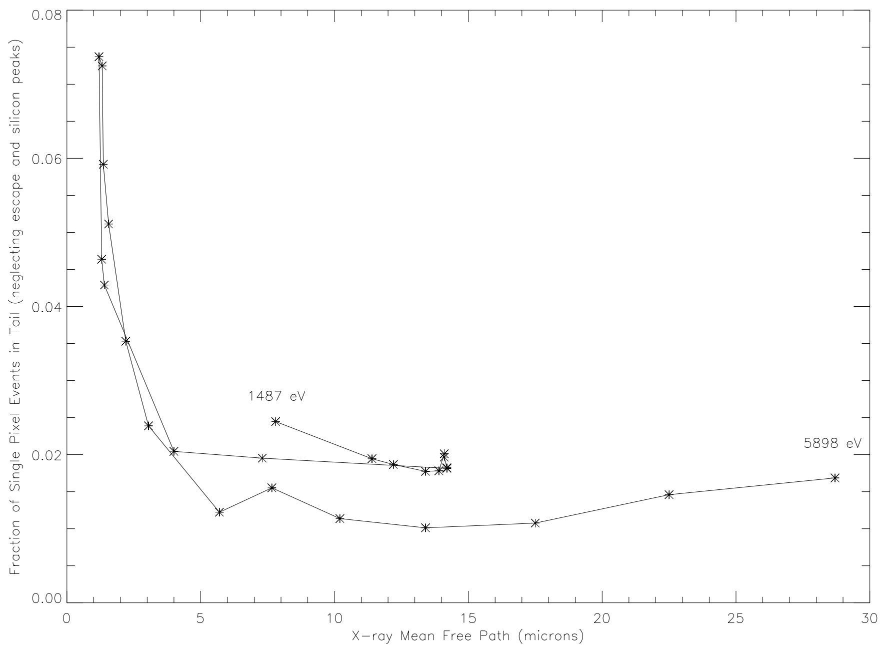

Figure 1.14: Fraction of single pixel events in tail as a function of characteristic absorption length in silicon.

calculations are shown on Fig. 1.15. The values of cloud sizes are significantly lower than 150 – 200 nm reported in [21, 23]. They also are much smaller than cloud sizes in the bulk silicon extracted from our mesh experiments [27]. We believe the reason for this large discrepancy is the presence of a potential barrier for electrons at the $Si - SiO_2$ interface.

Electron cloud generation starts with emission of relatively high energy primary photo- and Auger electrons which dissipate their energy in an ionization cascade. The range of electrons in the initial stages of the cascade is roughly consistent with the cloud radius in our model. It is the low energy, nearly thermalized electrons with sharply increased mean free path (of an order of 100 nm), that are responsible for the large cloud sizes quoted in [21, 23]. In the MOS structure analyzed here a "potential wall" at the $Si - SiO_2$ interface prevents the low energy electrons from penetrating into the SiO_2 for the clouds centered at a distance greater than R from this interface. Only hot electrons in the initial stages of cascading (for which the range is very small) can participate in the cloud splitting between the silicon and the silicon dioxide. This feature of the buried channel MOS X-ray CCDs is very beneficial for the spectrometric properties of the frontside illuminated CCDs, since it results in larger fraction of counts going into the main peak instead of the tail, and, hence, better energy resolution and quantum efficiency.

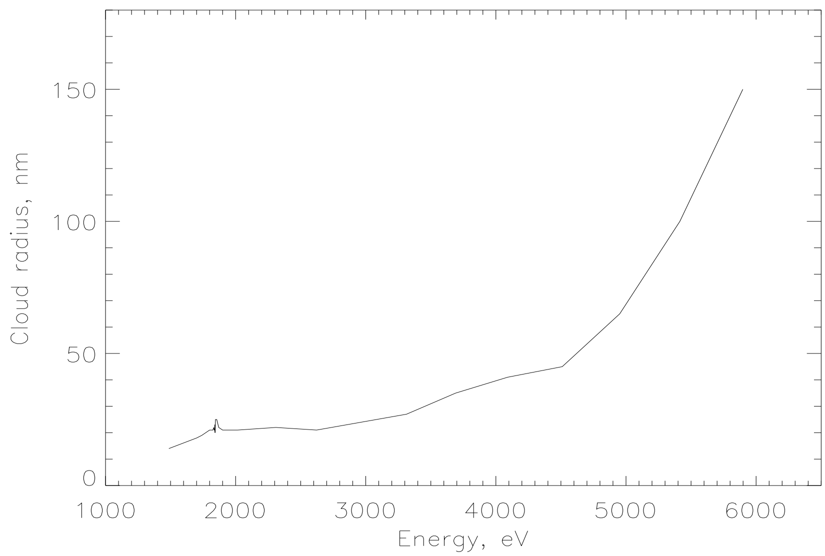

Figure 1.15: Cloud radius in silicon as a function of energy.

The precise shape of the tail depends on the density distribution of charge in the cloud and this distribution in principle can be extracted. We have not accomplished this task yet, because it requires much higher number of counts than we were able to obtain during the limited time at the synchrotron facility.

We have developed a model based on the scheme shown at Fig. 1.13. The basic assumption is that each electron cloud is a sphere and when the sphere crosses the silicon interface, the number of electrons produced in each material is proportional to the volume of the corresponding segment of the sphere. Each material is assumed to have different electron-hole creation energy. This is equivalent to assuming that electrons have the same mean free path in both materials. This may be not such a bad approximation, especially for high energy electrons in the original stages of cascading. As discussed above, electrons liberated in the oxide contribute to the total charge collected. From the low energy peak position (see Fig. 1.9) we deduce an effective electron-hole pair creation energy w_{ox} in SiO_2 of approximately 52 eV. This value includes recombination losses and hence differs significantly from the reported value of 17 eV/pair. We have made no attempt here to decouple the true value of w_{ox} and the losses. This matter is clearly worth pursuing, because it will allow to produce a more accurate model of the device response.

In Fig. 1.16 - 1.19 are shown the results of the best fit of the model to the data at several energies.

The results of the this section are used as the basis for the model of the CCD described

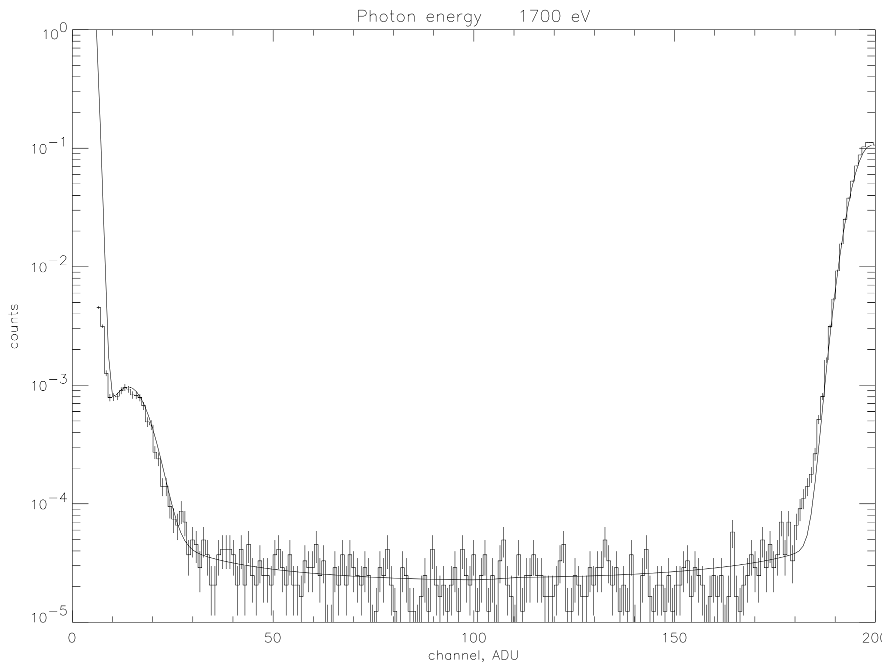

Figure 1.16: Response of the CCD to the 1700 eV photons and the model prediction.

in section 1.14 to produce a response matrix of the flight devices.

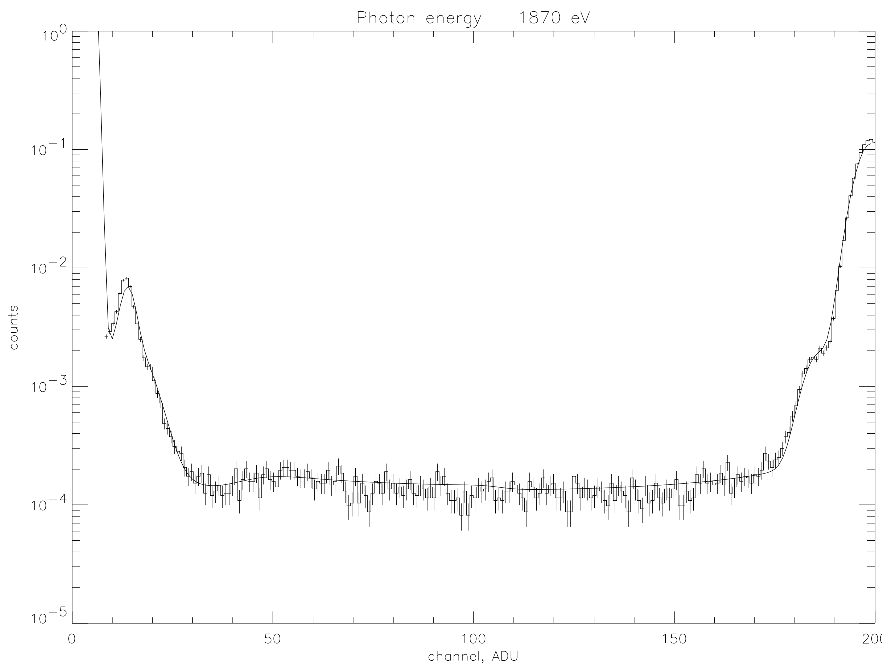

Figure 1.17: Response of the CCD to the 1870 eV photons and the model prediction.

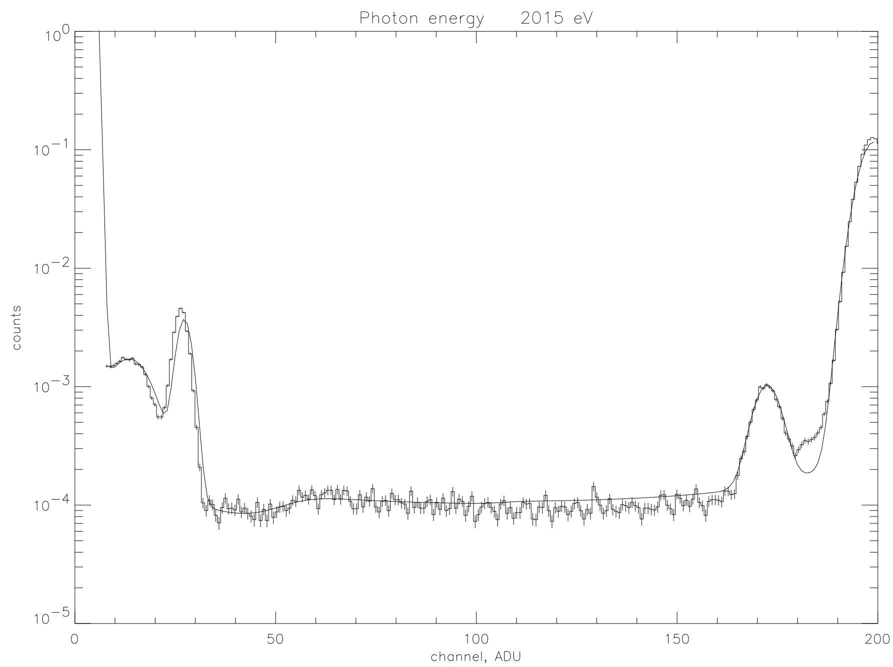

Figure 1.18: Response of the CCD to the 2015 eV photons and the model prediction.

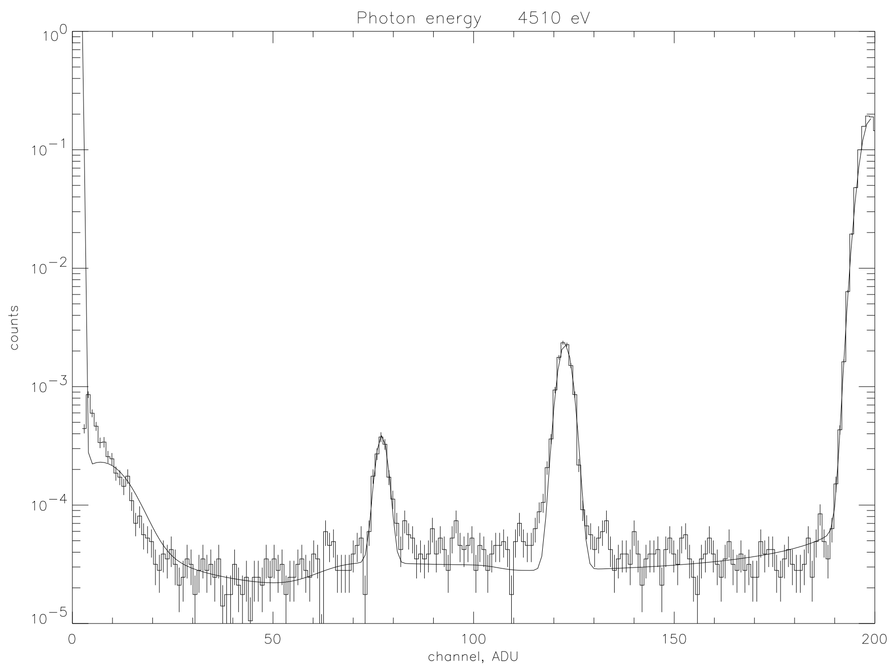

Figure 1.19: Response of the CCD to the 4510 eV photons and the model prediction.